Steroid hormones produced by coral-associated *Endozoicomonas* prime the coral immune response during thermal stress

Amin R. Mohamed[1,2$*], Michael A. Ochsenkühn[1$], Trent D. Haydon[3], Salah Abdelrazig[1], Lisa S.Y. Coe[1], Gabriel Mochales-Riaño[3], Woonkee S. Jo[4], Alan R. Healy[4], David Abrego[5,6], Jean-Baptiste Raina[7], John A. Burt[3,8,9], Shady A. Amin[1,3,9*]

[1]Marine Microbiomics Laboratory, New York University Abu Dhabi, Saadiyat Island, Abu Dhabi, United Arab Emirates

[2]Zoology Department, Faculty of Science, Benha University, Benha, Egypt

[3]Center for Genomics and Systems Biology, New York University Abu Dhabi, Saadiyat Island, Abu Dhabi, United Arab Emirates

[4]Chemistry Program, New York University Abu Dhabi (NYUAD), Saadiyat Island, United Arab Emirates

[5]Faculty of Science and Engineering, Southern Cross University, Coffs Harbor, NSW, Australia

[6]Lizard Island Research Station, Australian Museum, Sydney NSW, Australia

[7]Max Planck Institute for Marine Microbiology, Bremen, Germany

[8]Marine Biology Laboratory, New York University Abu Dhabi, Saadiyat Island, Abu Dhabi, United Arab Emirates

[9]Mubadala Arabian Center for Climate and Environmental Sciences, New York University Abu Dhabi, Saadiyat Island, Abu Dhabi, United Arab Emirates

[*]Corresponding Authors:

Shady A. Amin, Biology Program, New York University Abu Dhabi, Saadiyat Island, Abu Dhabi, United Arab Emirates. Email: samin@nyu.edu , Tel: (+971) 2 628 5743

Amin R. Mohamed, Biology Program, New York University Abu Dhabi, Saadiyat Island, Abu Dhabi, United Arab Emirates. Email: amin.mohamed@nyu.edu, Tel: (+971) 2 628 7863

[$]equally-contributed

Abstract

The coral microbiome is believed to play a critical role in sustaining corals and enabling adaptation to thermal stress. A ubiquitous group of coral-associated bacteria, known as *Endozoicomonas*, are hypothesized to provide essential metabolites to corals, though the exact roles these bacteria play during ambient or thermal stress conditions are largely unknown. We demonstrate that while *Endozoicomonas* synthesizes the iron-binding siderophore aerobactin *in vitro*, this trait may be suppressed *in hospite*. Integrated metagenomics, metabolomics, and lab validations reveal that within the coral holobiont *Endozoicomonas* is the only microbe capable of metabolizing coral-derived testosterone and converting ubiquitous cholesterol into testosterone and progesterone, important steroids that accumulate within the coral holobiont during thermal stress. Provision of testosterone and progesterone to corals during thermal stress induced transcriptional reprogramming of the coral innate immune response, promoting cellular survival and suggesting active microbial involvement in immune priming and stress resilience. These findings highlight a previously unrecognized mechanism of microbial contribution to coral resilience. Lastly, the capacity of bacteria to synthesize eukaryotic steroids implies deep evolutionary connections between microbial metabolism and the origin of steroid-mediated processes in early eukaryogenesis.

Keywords: coral symbiosis, *Endozoicomonas*, thermal stress, chemical diversity, steroids, siderophore.

Introduction

Corals form intricate associations with a diverse microbiome, collectively referred to as the coral holobiont[1]. This microbiome has been recognized as an essential contributor to coral health and resilience, especially during thermal stress[2–4]. While the symbiotic interactions between corals and their primary algal endosymbiont, Symbiodiniaceae, have been extensively studied[5–7], the functional roles of bacteria in the coral holobiont remain largely unexplored[2,8], despite their importance for coral health[3,9,10]. Among the myriad of bacteria associated with corals, the genus *Endozoicomonas* has received considerable attention due to its ubiquitous distribution across coral species and geographic locations[11–13] and the correlation between its abundance and coral health[11,14,15].

While *Endozoicomonas* are sometimes present in the coral mucus[16,17], they are primarily localized within coral tissues as cell-associated microbial aggregates (CAMAs)[18]. Based on genomic predictions, *Endozoicomonas* spp. are hypothesized to play a crucial role in coral holobiont metabolism through the recycling of essential nutrients and biosynthesis of B-vitamins, amino acids and organosulfur compounds[11,19–21]. Indeed, when exposed to coral tissue extracts, *E. marisrubri* activates vitamins B_1 and B_6 biosynthesis and glycolytic processes[22]. However, despite recent efforts[13,21,23–25], a definitive role for *Endozoicomonas* within the coral holobiont and the precise function underlying its symbiotic association is yet to be identified.

In this study, we combine multiomics data (16S rRNA gene amplicons, shotgun metagenomics, and untargeted metabolomics) to elucidate the functional roles of *Endozoicomonas* during coral response to extreme thermal conditions in the Arabian Gulf, the hottest sea on Earth with surface temperature exceeding 36°C[26]. To investigate symbiotic interactions in the coral holobiont, our sampling scheme included both healthy corals, representing stable host-microbiome associations, and corals infected with white syndrome, representing a dysbiotic state. Diseased samples, characterized by a marked reduction in the relative abundance of *Endozoicomonas*, provided a natural contrast to healthy corals that enabled us to determine the functional contribution of this taxon. By integrating metagenomic and metabolomic data, we uncover both shared and niche-specific metabolic pathways among members of the coral holobiont. Given the prominence of *Endozoicomonas* as a key member of the healthy coral microbiome, we leverage pangenomic analysis to delineate conserved and unique functions in *Endozoicomonas* lineages. We then perform additional experimental validations of these functional predictions.

We show that *Endozoicomonas* encodes genes for the biosynthesis and uptake of the iron-binding siderophore aerobactin, and confirm its ability to produce it *in vitro*, likely to access bioavailable

92 iron *ex hospite*. In addition, we show that during thermal stress, two terminal steroid hormones,
93 testosterone and progesterone, are abundant in corals despite the depletion of most of their
94 precursors. We reveal that *Endozoicomonas* is the only holobiont member to possess the gene
95 repertoire required for testosterone degradation and, surprisingly, can metabolize cholesterol to
96 produce progesterone and testosterone *in vitro*, a unique capability only present in select bacteria.
97 Finally, we show that progesterone and testosterone play a critical role in modulating the coral
98 immune response during thermal stress by promoting pro-survival signaling while suppressing
99 pro-inflammatory responses. These findings constitute a major breakthrough in our understanding
100 of bacterial contributions to coral resilience and host–microbe interactions.

101

102 **Results**

103 We monitored and sampled colonies of the coral *Acropora pharaonis*[27] for 16S rRNA gene
104 amplicons, shotgun metagenomics and untargeted metabolomics from Saadiyat reef on the
105 Arabian Gulf off the coast of Abu Dhabi. Sampling occurred across a temperature gradient starting
106 with early thermal stress showing preliminary signs of white syndrome disease on some colonies
107 at 32°C (June), severe thermal stress and further white syndrome progression at 34°C (August),
108 and recovery at 27°C (October) (Extended Data Table 1). Samples were collected from healthy
109 coral tissues at all three temperatures, and from dysbiotic controls (i.e., white-syndrome lesion
110 sites (L) and healthy appearing tissue adjacent to the lesion (AL)) at 34°C (Fig. 1a). All samples
111 were extracted for metabolites and genomic DNA to profile the coral holobiont metabolome and
112 microbiome composition and functional potential.

113 **Divergent metabolite and bacterial profiles in corals under extreme temperature**

114 The intracellular metabolites of the coral holobiont were extracted and analyzed with reverse
115 phase liquid chromatography-high resolution mass spectrometry (RP-LC/HRMS) in positive and
116 negative ionization modes and in tandem with MS^2 mass fragmentation. A total of 5878 putative
117 molecular features were predicted based on *in-silico* mass fragmentation network analysis
118 (SIRIUS) (*see* Methods; Supplementary Information Table 1). Principal component analysis (PCA)
119 patterns were significantly different (PERMANOVA; F-value = 7.58; R^2 = 0.62; adj. *p*-value=0.001)
120 and showed that early stress (32°C) and recovery (27°C) metabolomes clustered together away
121 from severe stress (34°C), suggesting that despite being separated by four months (June to
122 October) the holobiont metabolic state during early stress and recovery were similar (Fig. 2a;
123 Extended Data Fig. 1). The metabolomes of the diseased samples (L, AL) displayed inter-colony

variations and showed a significant separation from all other samples, suggesting a fundamentally different chemical composition compared to healthy tissue (Fig. 2a). These findings confirm that acroporid corals in the Arabian Gulf exhibit a notable tolerance to temperatures up to 32°C, lethal to corals elsewhere, while exposure to 34°C poses a critical challenge to their overall fitness, which aligns with previous reports[28].

The bacterial microbiome composition, based on 16S rRNA gene amplicons, revealed that disease samples (L, AL) differed significantly from all other samples (PERMANOVA; F-value = 1.98; R^2 = 0.0318; *adj.* p-value = 0.01), suggesting the bacterial microbiome is resilient and only undergoes a significant shift during disease progression (Fig. 2b). Thirty-two bacterial ASVs belonging to the family Endozoicomonadaceae dominated the microbiome, with an average relative abundance of 60% in healthy samples. In addition, Endozoicomonadaceae persisted under elevated (32°C) and even extreme temperatures (34°C), which was particularly remarkable as they usually disappear during coral exposure to thermal stress[29] (Fig. 2c; Extended Data Fig. 2a). At lesion sites, the relative abundance of Endozoicomonadaceae was only 1.3%, while Rhodobacteraceae and Saprospiraceae contributed 23% and 39% of the microbiome, respectively, indicating the proliferation of potentially opportunistic microbes at the expense of Endozoicomonadaceae during disease onset (Fig. 2c; Extended Data Fig. 2a)[30–32].

Integrated metagenome/metabolome analysis implicates the microbiome in steroid hormone metabolism

The metagenomes of coral holobionts produced a total of 589 gigabases (Gb), averaging 42 Gb per sample (Supplementary Information Table 3; Extended Data Fig. 3). We leveraged publicly available genomes for *Acropora* and *Cladocopium* to partition the holobiont metagenome before assembling coral and algal contigs (see Methods). A total of 257 million reads (~7% of the holobiont reads) were classified as microbial (i.e., non-coral, non-algal reads; Fig. 2d). These microbial reads were used for downstream read-based and assembly-based metagenomic analyses (Extended Data Fig. 2b and 3; Supplementary Information Table 3). Taxonomic profiling of putative metagenomic microbial reads revealed a diverse coral microbiome primarily dominated by bacteria, comprising 95% of the microbial community (Extended Data Fig. 2b). To explore the potential roles of the microbiome, we assigned all genes and putatively annotated metabolites in our metagenomic and metabolomic datasets to members of the coral holobiont. To do this, metagenomic reads assigned to host, algal symbiont or bacteria were assembled and functionally annotated using the KEGG database to a total of 11,333 KEGG Orthology terms[33] (KOs). While a third of the predicted KOs (3,065) were shared between different members of the holobiont, most

157 were uniquely assigned to the coral host (4,619), followed by microbes (3,029) and algal
158 symbionts (620) (Fig. 2e; Supplementary Information Table 4). Using these KO taxonomic
159 assignments, we mapped the putatively annotated metabolites associated with KEGG compounds
160 (284) (Supplementary Information Table 2). This analysis indicated 148 of these putative
161 metabolites were shared between different members of the holobiont, while 43 were assigned
162 uniquely to the host, 42 to the algal symbiont and 51 to other microbes (Fig. 2e, Extended Data
163 Table 2). Examining the KEGG pathways across metagenomes and metabolomes indicated that
164 the host dominates the biosynthesis of steroid hormones, retinol metabolism, and vitamin
165 digestion and absorption, while microbes dominate biosynthesis of cofactors, biosynthesis of
166 secondary metabolites, and steroid degradation (Fig. 2e).

167 To assign functions to specific bacterial taxa, we assembled genomes from our metagenomes
168 (MAGs). Coral samples devoid of mucus and seawater yielded 11 medium to high-quality MAGs
169 (completeness >75% and contamination <10%). Core microbiome members were defined as
170 MAGs consistently present at relatively high (40-60%) abundance in healthy tissues (at all
171 temperatures), but showing reduced abundance in dysbiotic samples (AL and L) (Fig. 3a). Out of
172 the 11 MAGs, two MAGs stood out as important members of the coral holobiont: MAG01 assigned
173 to the phylum Myxococcota and MAG10 assigned to the genus *Endozoicomonas* (Extended Data
174 Fig. 4; Supplementary Information Table 5). *Endozoicomonas* (MAG10; completeness: 91%,
175 contamination: 1.4%), exhibited a dynamic abundance profile as its relative abundance peaked at
176 32°C during early stress (65.4%), followed by a dramatic decrease at 34°C (35.8%) and then
177 bounced back with a modest abundance during recovery at 27°C (43%) (Fig. 3a). The relative
178 abundance of MAG10 dropped drastically in L samples (0.8%), coinciding with dysbiosis and
179 consistent with previous reports[30–32]. Given its dynamic abundance pattern and strong association
180 with healthy coral states, we next explored the functional potential of MAG10 to better understand
181 its role within the coral holobiont.

182

183 **Pangenome analysis reveals conserved functions across *Endozoicomonas* genomes**

184 Since culturing efforts of *Endozoicomonas* from *Acropora* in the Arabian Gulf were not successful,
185 we isolated *Endozoicomonas acroporae* AT381 from *A. kenti* from the Great Barrier Reef (GBR),
186 referred to hereafter as AT381 (Fig. 1b), and obtained a nearly complete genome (size = 6.02
187 Mbp; completeness = 99.1%) predicted to harbor 5001 coding sequences (CDS). AT381 and
188 MAG10 are closely related as they share an average nucleotide identity (ANI) of 94.3%[34].
189 Phylogenomic analysis between MAG10, AT381 and 27 publicly available *Endozoicomonas*

190 genomes and MAGs from diverse invertebrate hosts further confirmed the close relationship
191 between MAG10, AT381 and other *E. acroporae* genomes (Extended Data Fig. 5). Functional
192 conservation and specialization across all *Endozoicomonas* genomes were examined by
193 constructing a pangenome of their 34,846 gene clusters (Fig. 3b, Supplementary Information
194 Table 6)[35]. Because of the inability to culture a MAG10 relative from the Arabian Gulf, we used
195 pangenomic analysis to confirm functional conservations within the *Endozoicomonas* genus and
196 further functionally validated some of these conserved capabilities using the closely related *E.*
197 *acroporae* AT381 from the GBR and two other *Endozoicomonas* isolates.

198 We hypothesized that *Endozoicomonas* genomes symbiotic with corals possess specialized, but
199 shared functions enabling interactions with their coral hosts, compared to genomes isolated from
200 other hosts. As reported for other genomes of coral-associated *Endozoicomonas* spp., MAG10
201 harbors genes related to symbiosis establishment, e.g., flagellar assembly, type IV pili[18], ankyrin
202 and tetratricopeptide repeats[21,22], several secretion systems involved in host infection (T2SS,
203 T3SS, T6SS)[18,21–23], complete biosynthesis pathways for the vitamins riboflavin (B_2), biotin (B_7)
204 and pyridoxal-phosphate (B_6), and nine essential amino acids and their transporters (Extended
205 Data Fig. 4b and c, Supplementary Information Table 7)[11]. MAG10 was also significantly enriched
206 within the holobiont for antioxidant production[22], heme biosynthesis[25], glycoside hydrolases that
207 cleave the most abundant marine polymers, starch and chitin[36], and diverse ABC transporters
208 (Supplementary Information Tables 7 and 8). In addition to these previously known functions,
209 MAG10 is capable of **(a)** catabolizing histidine to glutamate, an essential intermediate for
210 ammonium assimilation and a common feature of most *Endozoicomonas* genomes, **(b)** degrading
211 galactose (Leloir pathway), a Symbiodiniaceae photosynthate[37], which is a common feature in
212 most *Endozoicomonas* genomes, **(c)** biosynthesizing the nucleoside antibiotic showdomycin, **(d)**
213 biosynthesizing and exporting the polyamine spermidine, a reactive oxygen species scavenger,
214 and export proteins for its precursor putrescine, **(e)** and biosynthesizing ectoine, a bacterial
215 osmoprotectant (Fig. 3b, Extended Data Fig. 4c, Extended Data Tables 3 and 4, Supplementary
216 Information Table 7). Cumulatively, these functions may enhance symbiosis and increase the
217 fitness of the coral host and/or Symbiodiniaceae, especially during thermal stress.

218

219 ***Endozoicomonas* acquires iron *in vitro* using the siderophore aerobactin**

220 Siderophores are small molecules secreted by some bacteria and fungi to acquire iron in iron-
221 limited environments[38] and can play important roles in iron cycling and bioavailability in the pelagic

222 ocean[39,40]. The genome of *Klebsiella pneumoniae,* a model bacterium for studying the
223 biosynthesis of the siderophore aerobactin, possesses the canonical, complete gene
224 cluster/operon containing aerobactin synthases (*iucA/iucC*) and the TonB-dependent uptake
225 receptor (*iutA*) used to produce apo-aerobactin and take up Fe-bound aerobactin, respectively[41].
226 In contrast, MAG10, all other *E. acroporae* and 8 additional coral- and invertebrate-associated
227 *Endozoicomonas* genomes possessed only the biosynthesis genes within the gene cluster, while
228 having either a distal *iutA* that is outside of the gene cluster in the case of AT381 or a homolog of
229 *iutA* in a completely separate region of the genome for all other *Endozoicomonas* that possess
230 the gene cluster (Fig. 4a, Extended Data Table 4). Aerobactin requires a functional *iutA* for Fe
231 acquisition to function[42] and a distal *iutA* suggests a potential decoupling from biosynthesis. To
232 confirm whether *Endozoicomonas* can use aerobactin to acquire iron, we grew multiple strains *in*
233 *vitro* under Fe-limiting conditions and tested their siderophore production using the chrome azurol
234 S assay (CAS)[43]. The tested strains include two isolates from *Acropora*: *E. acroporae* AT381 and
235 *E. acroporae* Acr14*,* and *E. montiporae* CL33 (isolated from *Montipora*), a negative control that
236 lacks aerobactin biosynthesis genes (Extended Data Table 4). The CAS assay showed that *E.*
237 *acroporae* AT381 and Acr14 were able to grow and utilize Fe from CAS (Fig. 4b) while *E.*
238 *montiporae* was not able to grow, consistent with its inability to produce aerobactin. These findings
239 suggest that select *Endozoicomonas* strains and species (12 out of 27 in total) can utilize
240 siderophores for Fe acquisition *in vitro* and likely *ex hospite*. We were not able to detect any m/z
241 signatures that match aerobactin, its Fe-complex or photoproducts[44] in the holobiont
242 metabolomes. Indeed, siderophore production *in hospite* is mainly associated with pathogenic
243 bacteria[45], and siderophore production may take place when *Endozoicomonas* are in seawater *ex*
244 *hospite*.

245 The fact that all examined *Endozoicomonas* genomes capable of biosynthesizing aerobactin
246 possess distal, not proximal, *iutA* homologs indicates a potential decoupling of expression
247 between biosynthesis and transport, which can make Fe acquisition less efficient and more
248 energetically costly for the bacteria. This pattern also suggests a gradual loss of function of the
249 transporter that would eventually abolish aerobactin biosynthesis over evolutionary timescale.
250 Indeed, a loss of function was concluded from the lack of *iutA* in the genomes of *Bacillus*
251 *licheniformis* and *B. halodurans* despite the presence of the aerobactin biosynthesis operon[46].

252 To assess the evolutionary pressures acting on the *iutA* gene, we calculated rates of non-
253 synonymous and synonymous substitutions (dN/dS) ratios across multiple *E. acroporae* strains
254 compared to the housekeeping gene DNA Polymerase III subunit delta as a conserved core gene

255 against *E. acroporae* AT381 as a reference (Supplementary Information Table 9). Several
256 *Endozoicomonas* isolates from *Acropora* displayed signatures of relaxed purifying selection
257 (significantly elevated dN/dS) in *iutA*, suggesting ecological redundancy or diminished reliance on
258 siderophore-mediated iron acquisition in certain niches. In contrast, *iutA* in *E. acroporae* Acr14
259 exhibited low dN/dS value (0.1), consistent with strong purifying selection and functional
260 conservation. These patterns suggest that while some *Endozoicomonas* strains may reduce
261 dependence on siderophore systems, others retain this capability, potentially as a survival strategy
262 during transitions to a free-living lifestyle *ex hospite*. MAG10 was not included in this analysis
263 because MAGs are typically a mosaic of sequences from multiple closely related strains, rather
264 than a single, clonal genome. This chimerism, along with assembly artifacts, can distort
265 substitution rate estimates and obscure true evolutionary signals[47], a concern that is particularly
266 relevant here given the high strain-level diversity we observed, with 32 distinct ASVs from
267 Endozoicomonadaceae identified by 16S rRNA gene amplicon sequencing. Thus, we propose
268 that coral-associated *Endozoicomonas* do not utilize siderophore-mediated iron uptake *in hospite*,
269 a function that could be used in the free-living stage, and that over evolutionary time aerobactin-
270 dependent Fe acquisition will be lost. Coral-associated *Endozoicomonas* can instead utilize other
271 pathways to acquire iron, such as heme transporters (Supplementary Information Table 7).

272

273 **Steroid metabolism is a prominent function of *Endozoicomonas* among the coral**
274 **microbiome**

275 MAG10 was the only holobiont member that possessed the complete pathway to utilize carbon
276 from the degradation of the steroid hormone testosterone via 3-oxosteroid 1-dehydrogenase
277 (*kstD*) gene (Fig. 5a,b; Supplementary Information Table 4, 7; Extended Data Fig. 3). This function
278 was shared with most *Endozoicomonas* genomes (Fig. 3b; Extended Data Table 4), consistent
279 with their broader capacity to break down this important steroid molecule[48]. The relative
280 abundance of most steroids gradually and significantly decreased as temperature increased, with
281 abundance at 34°C, AL, and L near background levels (Fig. 5a, Extended Data Fig. 6,
282 Supplementary Information Table 9), consistent with previous reports[49,50] showing suppression of
283 steroid hormone production under stress and during infection. Surprisingly, a notable exception to
284 this pattern were select key terminal steroids and steroid degradation products. Specifically, the
285 putative eukaryotic hormones, progesterone, testosterone and estradiol-17β, in addition to
286 *Endozoicomonas*-derived androsta-1,4-diene-3,17-dione and HIP showed the highest relative
287 abundance at 34°C, with most other samples at near background levels (Fig. 5a, Supplementary

288 Information Table 10). Since the sampling timepoints fell outside the spawning season in the
289 Arabian Gulf (March to May)[51], and most precursors of progesterone and testosterone showed
290 low relative abundance near background levels at 34°C, the elevated levels of these putative
291 steroid hormones during severe stress at 34°C were unexpected. Since these precursors are
292 required for the synthesis of testosterone and progesterone, their absence suggests they are
293 either depleted by the host or a source other than the host, is providing testosterone and
294 progesterone. Notably, MAG10 was the only microbiome member that possessed a 17-β-
295 hydroxysteroid dehydrogenase (K05296; E1.1.1.51) that synthesizes testosterone from
296 androstenedione, the reverse reaction of KstD (Supplementary Information Table 7)[52]. Therefore,
297 we hypothesized that *Endozoicomonas* may provide corals with some of these steroids during
298 severe stress.

299

300 MAG10 and other *Endozoicomonas* genomes (e.g., *E. montiporae*) encode genes associated with
301 cholesterol binding, such as those containing the steroidogenic acute regulatory protein-related
302 lipid transfer (START) and sterol carrier protein-2 (SCP2) domains, as well as
303 cholesterol/phospholipid transport, including MlaD, MlaE, and ABC transporters (Supplementary
304 Information Table 7). Therefore, we investigated whether *Endozoicomonas* can catabolise
305 testosterone, convert androstenedione to testosterone and if it synthesizes the terminal steroids
306 progesterone, testosterone, or estradiol-17β from cholesterol, given that cholesterol is the
307 precursor of steroid hormones and can be one of the abundant steroid molecules in the coral
308 holobiont[48,53]. Cultures of three *Endozoicomonas* strains, *E. acroporae* AT381, *E. acroporae* Acr14
309 and *E. montiporae* were grown at 26°C and 34°C in minimal media with or without cholesterol,
310 testosterone or androstenedione (Fig. 1b). After 24 hours, all three strains catabolized
311 testosterone into androstenedione and downstream metabolites leading to the TCA cycle, with *E.*
312 *acroporae* Acr14 only carrying out this transformation at 34°C, while *E. acroporae* AT381 and *E.*
313 *montiporae* doing so at both temperatures (Fig. 5c, Supplementary Information Table 11),
314 suggesting thermal regulation of these transformations in *E. acroporae* Acr14. All three strains
315 were also able to convert androstenedione to testosterone at both temperatures likely via 17-β-
316 hydroxysteroid dehydrogenase (Fig. 5d, Supplementary Information Table 11). Surprisingly, all
317 three strains were capable of transforming cholesterol into terminal steroids. *E. acroporae* AT381
318 converted cholesterol into the terminal products progesterone, testosterone, androstenedione and
319 other intermediates at both temperatures (Fig. 5e, Extended Data Fig. 6c). Conversely, *E.*
320 *acroporae* Acr14 converted cholesterol to cholesterol derivatives and progesterone only at 34°C

321 with no transformations observed at 26°C. Finally, *E. montiporae* converted cholesterol to
322 androstenedione, testosterone and related metabolites only at 26°C and switched to converting
323 cholesterol to cholesterol derivatives and progesterone at 34°C, indicating a strong temperature
324 influence on the regulation of these transformations (Fig. 5e). These findings suggest that
325 depending on the species/strain of *Endozoicomonas*, cholesterol conversion towards testosterone
326 or progesterone is controlled by temperature, which may explain the high relative abundance of
327 progesterone and testosterone in the holobiont at 34°C (Fig. 5 and Extended Data Fig. 6a,b).

328 Using high-resolution mass spectrometry and fragmentation information, we propose a metabolic
329 pathway that bifurcates cholesterol into **(a)** progesterone via pregnenolone and **(b)** testosterone
330 via oxo-cholestenoate and androstenedione (Fig. 5f). Although the *Endozoicomonas* pangenome
331 and auto-annotation highlight important enzymes for steroid degradation (e.g. *kstD*), further mining
332 of the *E. montiporae* genome yielded steroid delta isomerases of the CyP450 family, which
333 putatively convert pregnenolone into progesterone (Fig. 5f; Supplementary Information Table 7)[48].
334 MAG10 also encodes a member of the 3-beta hydroxysteroid dehydrogenase/isomerase protein
335 family [PF01073.22] (Supplementary Information Table 7). Orthologs of this protein are present in
336 all three *Endozoicomonas* strains we used for steroid incubations. This enzyme family includes
337 3β-hydroxysteroid dehydrogenase/Δ^5-Δ^4 isomerases (3β-HSDs), which plays a central role in
338 steroid biosynthesis by catalyzing the oxidation and isomerization of steroid precursors into active
339 steroid hormones. Although mining *Endozoicomonas* genomes did not reveal any specific
340 exporters for testosterone or progesterone, both hormones are lipophilic and can diffuse freely
341 through the cytoplasmic membrane[54–56]. Collectively, these findings indicate that *Endozoicomonas*
342 possess the genetic repertoire not only for steroid degradation, but for their conversion too,
343 positioning them as active contributors to steroid metabolism in the coral holobiont and suggesting
344 that these steroids play an integral role in the coral response to thermal stress. Because
345 testosterone is an immunosuppressive substrate under stress and progesterone is an
346 immunomodulatory and anti-inflammatory substrate in various animal models, we hypothesized
347 that the production of these hormones by *Endozoicomonas* likely modulates how the coral immune
348 system responds to thermal stress.

349 **Steroid hormones prime the coral immune response during thermal stress**

350 To determine whether corals can take up exogenous steroid hormones and their effective
351 concentrations, we incubated *Acropora* nubbins with three different concentrations of ^{13}C-labeled
352 testosterone (10 nM, 100 nM, 1 μM) for 48 hours and examined its relative abundance after 24
353 and 48 hours (Fig. 6a). While corals incubated with 1μM accumulated the most testosterone after

354 24 hours, the steroid relative abundance was highly reduced (3-fold) at 48 hours, suggesting
355 saturation. Similar results were obtained with incubations with 100 nM testosterone. At 10 nM,
356 *Acropora* accumulated testosterone progressively at 24 and 48 hours, resulting in an 11-fold
357 increase indicative of active uptake and limited metabolic removal, consistent with a potential
358 biological role; therefore, we used this concentration for subsequent experiments for both
359 testosterone and progesterone. To test the effect of each molecule on the immune response of
360 *Acropora,* coral nubbins were incubated with each molecule for 3 hours at an ambient temperature
361 of 28°C (T1), followed by an increase in temperature to 33°C (T2), simulating thermal stress and
362 at which point a second dose of progesterone or testosterone were added. To map the coral
363 immune system response to these steroids during thermal stress, samples were collected at T1,
364 T2 and at 24 hours post T1 (T3) (Fig. 6b) for RNA sequencing. Coral fragments were monitored
365 by measuring algal symbiont's photosynthetic efficiency (*Fv/Fm)* to ensure corals were stable and
366 exposure to both steroid hormones did not lead to physiological toxicity (Fig. 6c).

367 To examine differential expression of immune-related genes upon coral exposure to testosterone
368 or progesterone during thermal stress relative to untreated controls (Supplementary Information
369 Table 12, 13, 14), we compiled a list of all known innate immunity-related genes from our
370 assembled transcriptome (Fig. 6d). While many immune-related genes were activated due to heat
371 stress, exposure to testosterone or progesterone further increased their transcription (Fig. 6d,e).
372 For example during T2, both testosterone and progesterone treatments caused on average an
373 increase in the fold-change expression of master regulators of innate immunity, including tumor
374 necrosis factor receptor (TNFR; +129%), nuclear factor kappa B (NF-κB; +80%), and activator
375 protein 1 (AP-1; +10%) relative to controls, indicating increased immune signal transduction and
376 immune priming. Concomitantly, upstream immune-sensing and adaptor pathways (e.g., RIG1
377 and *TRAF2*; +131%, +1.9% respectively), as well as downstream genes linked to immune
378 regulation and anti-apoptosis (e.g., *TNFAIP3*, *BIRC2/3, BCL2*; +18.5%, +64%, +104%
379 respectively) were activated. This suggests that both testosterone and progesterone prime the
380 coral innate immune system during thermal stress by enhancing immune signaling and activating
381 both upstream sensing and downstream protective genes. Expression of pro-inflammatory
382 signaling components decreased (*TRAF6*; -32% and the JAK/STAT receptor *DOME*; -84%),
383 indicating immune-dampening that limits immune overreaction. Despite these shared effects in
384 the presence of testosterone and progesterone, progesterone uniquely enhanced transcriptional
385 responses associated with cell survival and anti-apoptotic signaling (*MCL1, BIRC4, PIM1*; +25%,
386 +161%, +245% respectively) and preferentially promoted negative feedback regulation of
387 cytokine-activated JAK/STAT pathway (*CISH/SOCS2*; +190%), consistent with suppression of

388 prolonged or excessive immune activation (Fig. 6d,e). Coincidentally, progesterone was
389 preferentially produced by some *Endozoicomonas* from cholesterol only during temperatures
390 resembling thermal stress (Fig. 5e), suggesting *Endozoicomonas* modulates the coral immune
391 system to suppress prolonged inflammatory responses to thermal stress.

392

393 **Discussion**

394 Despite the central role of microbial associates to coral health and fitness, the functional
395 mechanisms bacteria utilize to influence host physiology remain largely unresolved. Here, we
396 provide the first evidence that ubiquitous *Endozoicomonas* possesses an unexpected capacity to
397 synthesize terminal eukaryotic steroid hormones, a novel metabolic capability in the coral
398 microbiome, and that these hormones modulate the host immune response during thermal stress,
399 suggesting a critical functional role for this genus within the coral holobiont. Particularly, the ability
400 of *Endozoicomonas* to synthesize testosterone and progesterone in a temperature-dependent
401 manner confirms that their accumulation in the holobiont when seawater temperature is high may
402 be partially or wholly driven by *Endozoicomonas* symbionts. While steroid degradation is
403 widespread in many alpha- and gamma-proteobacteria[48,57,58], the ability to synthesize terminal,
404 host-active steroid hormones from cholesterol is rare and positions *Endozoicomonas* as a
405 metabolic outlier among coral symbionts. Specific human gut microbiota, such as *Bacteroides*
406 *acidifaciens* and *Ruminococcus gnavus*, synthesize steroid hormones and play a major role in
407 steroid hormone homeostasis in mammals[59]. Moreover, *Mycobacterium smegmatis* was shown to
408 synthesize testosterone and estrogens *in vitro* from steroid precursors[60]. While the mycobacterial
409 conversion of cholesterol to testosterone has been observed under fermentative conditions,
410 *Endozoicomonas* differs in its ability to carry these transformations under aerobic conditions,
411 highlighting a distinct biochemical strategy that can influence major functions in their host.

412 While steroid hormones play critical roles in many physiological functions, such as growth,
413 reproduction, and development in vertebrates[48], their role and origin in invertebrates have been
414 subject to recent debate[61]. While definitive CYP19A1 and HSD17B3 orthologs (the vertebrate
415 enzymes that catalyze the final steps in estrogen and androgen synthesis, respectively) have not
416 been identified in invertebrate genomes, several studies have demonstrated functional aromatase
417 activity in corals (e.g., *Euphyllia ancora*, *Pocillopora damicornis*) using substrate conversion
418 assays and inhibition by vertebrate aromatase inhibitors[62,63] that suggest invertebrates are capable
419 of synthesizing these molecules. We also identified several coral genes involved in steroid

420 hormone biosynthesis (Supplementary Information Table 7), including 17β-hydroxysteroid
421 dehydrogenase and several members of the cytochrome P450 enzyme family that can
422 biosynthesize testosterone and progesterone, respectively, as reported in previous coral
423 genomes[64]. This suggests that although the exact gene homologs that produce steroid hormones
424 may differ, the enzyme function is present.

425 In corals, steroid hormones play important roles in gametogenesis and spawning and exogenous
426 additions of steroid hormones influence the coral microbiome composition[61,65,66]. Our findings
427 indicate that, in addition to these functions, steroid hormones modulate the immune response to
428 thermal stress within hours of progesterone or testosterone addition. Specifically, hormone
429 exposure under thermal stress preferentially engaged TRAF2-associated TNF/NFKappaB
430 signaling and upregulated immune negative regulators, suggesting a survival-oriented, immune-
431 modulating state rather than a canonical inflammation response. TRAF signaling can diverge
432 toward either pro-survival or pro-inflammatory outcomes, with TRAF2 typically implicated in cell
433 survival and anti-apoptotic signaling[67] and TRAF6 commonly associated with inflammatory
434 pathways[68]. Indeed, exposure to either progesterone or testosterone under thermal stress induced
435 TRAF2 expression while suppressing TRAF6, suggesting a shift from inflammatory to anti-
436 apoptotic response relative to the coral's response under thermal stress alone (Fig. 6e). In
437 contrast to the combined steroid hormone response, progesterone uniquely attenuated the
438 JAK/STAT signaling pathway by downregulating DOME receptors and inducing the negative
439 regulators of JAK/STAT, CIS and SOCS (Fig. 6e). These patterns may fine-tune the immune
440 response by limiting immune overactivation while preserving basal immune competence[69,70]. By
441 priming innate immunity while constraining excessive inflammation, progesterone may help
442 balance pathogen defense with tissue protection, enhancing resistance to opportunistic microbes
443 without exacerbating heat-induced cellular damage or algal symbiont loss[71,72]. This balance may
444 be further fine-tuned by the temperature-sensitive regulation of steroidogenic biosynthesis
445 pathways in *Endozoicomonas* (Fig. 5), which may exert a disproportionate influence on holobiont
446 physiology relative to its abundance during thermal stress. Given the deep evolutionary
447 conservation of innate immune pathways in cnidarians[73,74], bacterially-derived steroid-based
448 signaling may represent an underappreciated metabolic interface between bacteria and early
449 diverging metazoa that contributes to the evolution of metazoa-microbe associations.

450

451 **Conclusion**

452 Recent evidence suggests the origin of protosteroids occurred up to 1.6 billion years ago[75],
453 coinciding with the proposed evolution of unicellular eukaryotes. This correlation indicates that the
454 origin of these molecules is most likely eukaryotic, especially given their role in sexual
455 reproduction, which is absent in prokaryotes. Through interkingdom interactions, some bacteria
456 might have inherited select genes from steroid hormone biosynthesis that enabled them to hijack
457 their host immune system and thus pave the way for establishing symbiotic interactions. The
458 limited distribution of this function across bacterial taxa associating with higher organisms
459 suggests these microbes occupy a unique niche that distinguishes them from other microbiome
460 members. Because of this selectivity, it may be that bacteria, such as *Endozoicomonas* that can
461 synthesize steroid hormones, may exert a disproportionate influence on holobiont physiology
462 compared to other bacteria. In the absence of *Endozoicomonas* during temperature-driven
463 disease[76], depletion of steroid precursors or reduced hormone availability may compromise host
464 immune regulation, creating favorable conditions for opportunistic pathogens to proliferate. Our
465 work reveals the unusual metabolic capabilities of coral-associated *Endozoicomonas* and the
466 functional role of this bacterial genus in the coral holobiont during heat stress, as they prime the
467 immune system of their hosts to withstand stressful events. We therefore propose a broader role
468 for steroids in the coral holobiont and highlight the significance of understanding coral symbiosis
469 in efforts to protect endangered coral reef habitats in a changing climate.

470 **Data Availability**

471 Metagenomic reads of the coral holobiont community consortium are deposited in NCBI under the
472 BioProject PRJNA1001615. Metagenomically assembled genomes and their annotations are
473 available on Zenodo (https://zenodo.org/records/15276884). The untargeted mass spectrometry
474 data is deposited on the Global Natural Products Social Molecular Network server
475 (https://gnps.ucsd.edu/) as raw data and can be accessed under the accession numbers
476 MSV000092488 and MSV000097641. Raw 16S rRNA gene amplicon libraries are deposited
477 under the BioProject PRJNA1262123 in NCBI. Raw sequences and reference genome for *E.*
478 *acroporae* AT381 are deposited under the accession number PRJNA1267713. Raw
479 transcriptomic sequences of the coral are deposited under the accession number PRJNA1414119.
480 *De novo*-assembled transcriptome, annotations, raw and normalised expression matrices are
481 provided under the Zenodo record number 18379496.

482 **Acknowledgements**

483 This work was supported by a Tamkeen award to S.A.A. (AD179) and by the NYUAD Research
484 Institute grants ADHPG-CGSB and CG009 to the Center for Genomics and Systems Biology

(CGSB) and Mubadala ACCESS, respectively. The authors acknowledge the NYU Abu Dhabi Core Technology Platform facilities for access to mass spectrometry facilities and boats for sampling. This research was carried out on the High-Performance Computing resources at New York University Abu Dhabi. Figure 1 and 6e were created using https://www.biorender.com.

Author contributions

MAO, DA and SAA conceived the project; MAO, TDH and DA conducted the sampling; MAO, TDH, LSYC, WJ and ARH processed the samples; TDH, SA, MAO, and JBR conducted lab experiments; AM, SA, MAO, WSJ, ARH and GMR carried out data processing and analysis; AM, MAO and SAA drafted the manuscript; AM, TDH, WSJ, SAA and MAO plotted all the figures; all authors contributed to manuscript preparation; SAA and JAB acquired funding for the project.

Competing Interest Declaration

The authors declare no competing interests.

Additional information

This paper is accompanied by extended data and Supplementary Information.

499 **References**

500 1. Rohwer, F., Seguritan, V., Azam, F. & Knowlton, N. Diversity and distribution of coral-associated
501 bacteria. *Mar. Ecol. Prog. Ser.* **243**, 1–10 (2002).
502 2. Bourne, D. G., Morrow, K. M. & Webster, N. S. Insights into the Coral Microbiome: Underpinning the
503 Health and Resilience of Reef Ecosystems. *Annu. Rev. Microbiol.* **70**, 317–340 (2016).
504 3. Ziegler, M. *et al.* Coral bacterial community structure responds to environmental change in a host-
505 specific manner. *Nat. Commun.* **10**, 3092 (2019).
506 4. Li, J. *et al.* Cultured Bacteria Provide Insight into the Functional Potential of the Coral-Associated
507 Microbiome. *mSystems* **7**, e00327-22 (2022).
508 5. Davy, S. K., Allemand, D. & Weis, V. M. Cell Biology of Cnidarian-Dinoflagellate Symbiosis. *Microbiol.*
509 *Mol. Biol. Rev.* **76**, 229–261 (2012).
510 6. LaJeunesse, T. C. *et al.* Systematic Revision of Symbiodiniaceae Highlights the Antiquity and
511 Diversity of Coral Endosymbionts. *Curr. Biol.* **28**, 2570-2580.e6 (2018).
512 7. Weis, V. M. Cell Biology of Coral Symbiosis: Foundational Study Can Inform Solutions to the Coral
513 Reef Crisis. *Integr. Comp. Biol.* **59**, 845–855 (2019).
514 8. Mohamed, A. R., Ochsenkühn, M. A., Kazlak, A. M., Moustafa, A. & Amin, S. A. The coral
515 microbiome: towards an understanding of the molecular mechanisms of coral–microbiota interactions.
516 *FEMS Microbiol. Rev.* **47**, fuad005 (2023).
517 9. Meunier, V. *et al.* Microbes support enhanced nitrogen requirements of coral holobionts in a high CO_2
518 environment. *Mol. Ecol.* **30**, 5888–5899 (2021).
519 10. Voolstra, C. R. & Ziegler, M. Adapting with Microbial Help: Microbiome Flexibility Facilitates Rapid
520 Responses to Environmental Change. *BioEssays* **42**, 2000004 (2020).
521 11. Neave, M. J., Michell, C. T., Apprill, A. & Voolstra, C. R. Endozoicomonas genomes reveal functional
522 adaptation and plasticity in bacterial strains symbiotically associated with diverse marine hosts. *Sci.*
523 *Rep.* **7**, 40579 (2017).
524 12. Ziegler, M., Seneca, F. O., Yum, L. K., Palumbi, S. R. & Voolstra, C. R. Bacterial community
525 dynamics are linked to patterns of coral heat tolerance. *Nat. Commun.* **8**, 1–8 (2017).
526 13. Pogoreutz, C. *et al.* Dominance of *Endozoicomonas* bacteria throughout coral bleaching and mortality
527 suggests structural inflexibility of the *Pocillopora verrucosa* microbiome. *Ecol. Evol.* **8**, 2240–2252

(2018).

14. Bayer, T. *et al.* The Microbiome of the Red Sea Coral Stylophora pistillata Is Dominated by Tissue-Associated Endozoicomonas Bacteria. *Appl. Environ. Microbiol.* **79**, 4759–4762 (2013).
15. Roder, C., Bayer, T., Aranda, M., Kruse, M. & Voolstra, C. R. Microbiome structure of the fungid coral *C tenactis echinata* aligns with environmental differences. *Mol. Ecol.* **24**, 3501–3511 (2015).
16. Pollock, F. J. *et al.* Coral-associated bacteria demonstrate phylosymbiosis and cophylogeny. *Nat. Commun.* **9**, 4921 (2018).
17. Apprill, A., Weber, L. G. & Santoro, A. E. Distinguishing between Microbial Habitats Unravels Ecological Complexity in Coral Microbiomes. *mSystems* **1**, e00143-16 (2016).
18. Maire, J. *et al.* Colocalization and potential interactions of *Endozoicomonas* and chlamydiae in microbial aggregates of the coral *Pocillopora acuta*. *Sci. Adv.* **9**, eadg0773 (2023).
19. Raina, J.-B. *et al.* DMSP biosynthesis by an animal and its role in coral thermal stress response. *Nature* **502**, 677–80 (2013).
20. Robbins, S. J. *et al.* A genomic view of the reef-building coral Porites lutea and its microbial symbionts. *Nat. Microbiol.* **4**, 2090–2100 (2019).
21. Tandon, K. *et al.* Comparative genomics: Dominant coral-bacterium Endozoicomonas acroporae metabolizes dimethylsulfoniopropionate (DMSP). *ISME J.* **14**, 1290–1303 (2020).
22. Pogoreutz, C. *et al.* Coral holobiont cues prime Endozoicomonas for a symbiotic lifestyle. *ISME J.* **16**, 1883–1895 (2022).
23. Wada, N. *et al.* High-resolution spatial and genomic characterization of coral-associated microbial aggregates in the coral *Stylophora pistillata*. *Sci. Adv.* **8**, eabo2431 (2022).
24. Maire, J. & Van Oppen, M. J. H. A role for bacterial experimental evolution in coral bleaching mitigation? *Trends Microbiol.* **30**, 217–228 (2022).
25. Hochart, C. *et al.* Ecology of Endozoicomonadaceae in three coral genera across the Pacific Ocean. *Nat. Commun.* **14**, 3037 (2023).
26. Nesterov, O. *et al.* Validation and statistical analysis of the Group for High Resolution Sea Surface Temperature data in the Arabian Gulf. *Oceanologia* **63**, 497–515 (2021).
27. Riegl, B. M., Benzoni, F., Samimi-Namin, K. & Sheppard, C. The Hermatypic Scleractinian (Hard) Coral Fauna of the Gulf. in *Coral Reefs of the Gulf* (eds. Riegl, B. M. & Purkis, S. J.) vol. 3 187–224

557 (Springer Netherlands, Dordrecht, 2012).
558 28. Howells, E. J., Vaughan, G. O., Work, T. M., Burt, J. A. & Abrego, D. Annual outbreaks of coral
559 disease coincide with extreme seasonal warming. *Coral Reefs* **39**, 771–781 (2020).
560 29. Marangon, E. *et al.* Destabilization of mutualistic interactions shapes the early heat stress response of
561 the coral holobiont. *Microbiome* **13**, 31 (2025).
562 30. Rosales, S. M. *et al.* A meta-analysis of the stony coral tissue loss disease microbiome finds key
563 bacteria in unaffected and lesion tissue in diseased colonies. *ISME Commun.* **3**, 19 (2023).
564 31. Becker, C. C., Brandt, M., Miller, C. A. & Apprill, A. Microbial bioindicators of Stony Coral Tissue Loss
565 Disease identified in corals and overlying waters using a rapid field-based sequencing approach.
566 *Environ. Microbiol.* **24**, 1166–1182 (2022).
567 32. Pollock, F. J., Wada, N., Torda, G., Willis, B. L. & Bourne, D. G. White Syndrome-Affected Corals
568 Have a Distinct Microbiome at Disease Lesion Fronts. *Appl. Environ. Microbiol.* **83**, e02799-16 (2017).
569 33. Kanehisa, M. KEGG: Kyoto Encyclopedia of Genes and Genomes. *Nucleic Acids Res.* **28**, 27–30
570 (2000).
571 34. Lee, I., Ouk Kim, Y., Park, S.-C. & Chun, J. OrthoANI: An improved algorithm and software for
572 calculating average nucleotide identity. *Int. J. Syst. Evol. Microbiol.* **66**, 1100–1103 (2016).
573 35. Eren, A. M. *et al.* Community-led, integrated, reproducible multi-omics with anvi'o. *Nat. Microbiol.* **6**,
574 3–6 (2020).
575 36. Keller-Costa, T. *et al.* Metagenomics-resolved genomics provides novel insights into chitin turnover,
576 metabolic specialization, and niche partitioning in the octocoral microbiome. *Microbiome* **10**, 151
577 (2022).
578 37. Ochsenkühn, M. A., Röthig, T., D'Angelo, C., Wiedenmann, J. & Voolstra, C. R. The role of floridoside
579 in osmoadaptation of coral-associated algal endosymbionts to high-salinity conditions. *Sci. Adv.* **3**,
580 e1602047 (2017).
581 38. Vraspir, J. M. & Butler, A. Chemistry of Marine Ligands and Siderophores. *Annu. Rev. Mar. Sci.* **1**,
582 43–63 (2009).
583 39. Barbeau, K., Rue, E. L., Bruland, K. W. & Butler, A. Photochemical cycling of iron in the surface
584 ocean mediated by microbial iron(iii)-binding ligands. *Nature* **413**, 409–413 (2001).
585 40. Amin, S. A. *et al.* Photolysis of iron–siderophore chelates promotes bacterial–algal mutualism. *Proc.*

586 *Natl. Acad. Sci.* **106**, 17071–17076 (2009).
587 41. Carbonetti, N. H. & Williams, P. H. A cluster of five genes specifying the aerobactin iron uptake
588 system of plasmid ColV-K30. *Infect. Immun.* **46**, 7–12 (1984).
589 42. Li, C. *et al.* Aerobactin-Mediated Iron Acquisition Enhances Biofilm Formation, Oxidative Stress
590 Resistance, and Virulence of Yersinia pseudotuberculosis. *Front. Microbiol.* **12**, 699913 (2021).
591 43. Schwyn, B. & Neilands, J. B. Universal chemical assay for the detection and determination of
592 siderophores. *Anal. Biochem.* **160**, 47–56 (1987).
593 44. Küpper, F. C., Carrano, C. J., Kuhn, J.-U. & Butler, A. Photoreactivity of Iron(III)−Aerobactin:
594 Photoproduct Structure and Iron(III) Coordination. *Inorg. Chem.* **45**, 6028–6033 (2006).
595 45. Miethke, M. & Marahiel, M. A. Siderophore-Based Iron Acquisition and Pathogen Control. *Microbiol.*
596 *Mol. Biol. Rev.* **71**, 413–451 (2007).
597 46. Rey, M. W. *et al.* Complete genome sequence of the industrial bacterium Bacillus licheniformis and
598 comparisons with closely related Bacillusspecies. *Genome Biol.* **5**, r77 (2004).
599 47. Meziti, A. *et al.* The Reliability of Metagenome-Assembled Genomes (MAGs) in Representing Natural
600 Populations: Insights from Comparing MAGs against Isolate Genomes Derived from the Same Fecal
601 Sample. *Appl. Environ. Microbiol.* **87**, e02593-20 (2021).
602 48. Ding, J.-Y., Shiu, J.-H., Chen, W.-M., Chiang, Y.-R. & Tang, S.-L. Genomic Insight into the Host–
603 Endosymbiont Relationship of Endozoicomonas montiporae CL-33T with its Coral Host. *Front.*
604 *Microbiol.* **7**, (2016).
605 49. Sun, F., Yang, H., Zhang, X. & Shi, Q. Metabolic and metatranscriptional characteristics of corals
606 bleaching induced by the most severe marine heatwaves in the South China Sea. *Sci. Total Environ.*
607 **858**, 160019 (2023).
608 50. Williams, A. *et al.* Multi-omic characterization of the thermal stress phenome in the stony coral
609 *Montipora capitata*. *PeerJ* **9**, e12335 (2021).
610 51. Howells, E. J., Abrego, D., Vaughan, G. O. & Burt, J. A. Coral spawning in the Gulf of Oman and
611 relationship to latitudinal variation in spawning season in the northwest Indian Ocean. *Sci. Rep.* **4**,
612 7484 (2014).
613 52. Sood, U., Singh, Y., Shakarad, M. & Lal, R. Highlight on Engineering *Mycobacterium smegmatis* for
614 testosterone production. *Microb. Biotechnol.* **10**, 73–75 (2017).

615 53. Hambleton, E. A. *et al.* Sterol transfer by atypical cholesterol-binding NPC2 proteins in coral-algal
616 symbiosis. *eLife* **8**, e43923 (2019).
617 54. Oren, A. Thermodynamic limits to microbial life at high salt concentrations. *Environ. Microbiol.* **13**,
618 1908–1923 (2011).
619 55. Walker, W. H. Testosterone signaling and the regulation of spermatogenesis. *Spermatogenesis* **1**,
620 116–120 (2011).
621 56. Carlson, J. C., Gruber, M. Y. & Thompson, J. E. A Study of the Interaction between Progesterone and
622 Membrane Lipids*. *Endocrinology* **113**, 190–194 (1983).
623 57. Bergstrand, L. H., Cardenas, E., Holert, J., Van Hamme, J. D. & Mohn, W. W. Delineation of Steroid-
624 Degrading Microorganisms through Comparative Genomic Analysis. *mBio* **7**, e00166-16 (2016).
625 58. Chiang, Y., Wei, S. T., Wang, P., Wu, P. & Yu, C. Microbial degradation of steroid sex hormones:
626 implications for environmental and ecological studies. *Microb. Biotechnol.* **13**, 926–949 (2020).
627 59. Arp, G. *et al.* Gut Bacteria Encode Reductases that Biotransform Steroid Hormones. Preprint at
628 https://doi.org/10.1101/2024.10.04.616736 (2024).
629 60. Dlugovitzky, D. G., Fontela, M. S., Martinel Lamas, D. J., Valdez, R. A. & Romano, M. C.
630 *Mycobacterium smegmatis* synthesizes in vitro androgens and estrogens from different steroid
631 precursors. *Can. J. Microbiol.* **61**, 451–455 (2015).
632 61. Tan, E. S. *et al.* Does estrogen regulate vitellogenin synthesis in corals? *Comp. Biochem. Physiol. A.*
633 *Mol. Integr. Physiol.* **255**, 110910 (2021).
634 62. Twan, W.-H., Hwang, J.-S. & Chang, C.-F. Sex Steroids in Scleractinian Coral, Euphyllia ancora:
635 Implication in Mass Spawning. *Biol. Reprod.* **2260**, 2255–2260 (2017).
636 63. Rougée, L. R. A., Richmond, R. H. & Collier, A. C. Molecular reproductive characteristics of the reef
637 coral Pocillopora damicornis. *Comp. Biochem. Physiol. A. Mol. Integr. Physiol.* **189**, 38–44 (2015).
638 64. Chiu, Y.-L., Shikina, S., Yoshioka, Y., Shinzato, C. & Chang, C.-F. De novo transcriptome assembly
639 from the gonads of a scleractinian coral, Euphyllia ancora: molecular mechanisms underlying
640 scleractinian gametogenesis. *BMC Genomics* **21**, 732 (2020).
641 65. Vilela, C. L. S. *et al.* Estrogen induces shift in abundances of specific groups of the coral microbiome.
642 *Sci. Rep.* **11**, 2767 (2021).
643 66. Twan, W.-H. *et al.* Hormones and reproduction in scleractinian corals. *Comp. Biochem. Physiol. A.*

644 *Mol. Integr. Physiol.* **144**, 247–253 (2006).
645 67. Petersen, S., Chen, T., Lawrence, D. et al. TRAF2 is a biologically important necroptosis suppressor.
646 Cell Death Differ 22, 1846–1857 (2015).
647 68. Mukundan L, Bishop GA, Head KZ, Zhang L, Wahl LM, Suttles J. TNF receptor-associated
648 factor 6 is an essential mediator of CD40-activated proinflammatory pathways in monocytes and
649 macrophages. J Immunol. 15;174(2):1081-90 (2005).
650 69. Amatya N, Garg AV, Gaffen SL. IL-17 Signaling: The Yin and the Yang. Trends Immunol.
651 38(5):310-322.(2017).
652 70. Kingsolver, MB & Hardy, R.W. Making connections in insect innate immunity, Proc. Natl. Acad.
653 Sci. U.S.A. 109 (46) 18639-18640 (2012).
654 71. Palmer CV. Immunity and the coral crisis. Commun Biol. 9;1:91. doi: 10.1038/s42003-018-0097-4
655 2018.
656 72. Virginia M Weis, Cell Biology of Coral Symbiosis: Foundational Study Can Inform Solutions to the
657 Coral Reef Crisis, Integrative and Comparative Biology, Volume 59, Issue 4, Pages 845–855 (2019).
658
659 73. Miller, D.J., Hemmrich, G., Ball, E.E. *et al*. The innate immune repertoire in Cnidaria - ancestral
660 complexity and stochastic gene loss. Genome Biol 8, R59 (2007).
661 74. Augustin R, Bosch TC. Cnidarian immunity: a tale of two barriers. Adv Exp Med Biol. 2010;708:1-
662 16.
663
664
665
666
667
668
669
670

671 **Main Figures and Figure Legends**

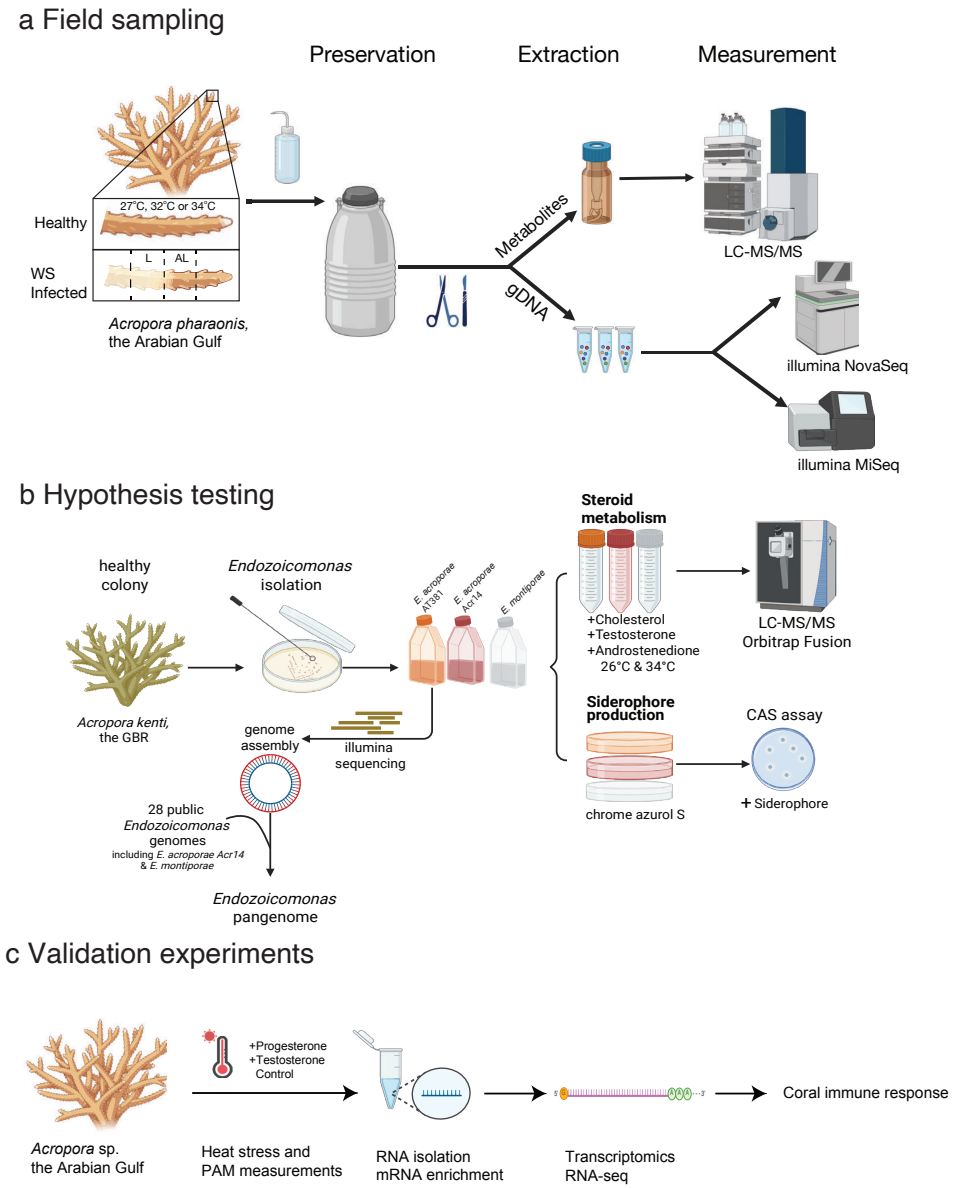

672

673 **Figure 1. Sampling, analysis, and validation experiments schemes**. **a**, *Acropora pharaonis*
674 colonies were sampled across a temperature gradient before gDNA and metabolites were
675 extracted for microbiome and metabolome analyses. Samples were collected during thermal
676 stress at 32°C and 34°C (June/August) and recovery at 27°C (October). Additional samples
677 showing white syndrome disease phenotypes at 34°C were also collected (L: lesion, AL:
678 adjacent to the lesion). Samples were processed for 16S rRNA gene amplicon, shotgun
679 metagenome, and untargeted metabolome analyses. **b**, To test the hypothesis derived from the
680 multiomics data, experiments were conducted on three coral coral-associated *Endozoicomonas*
681 to examine siderophore-mediated iron acquisition and steroid production. **c**, Transcriptomics
682 was then used to examine the effect of steroid hormones on the coral immune response during
683 thermal stress.

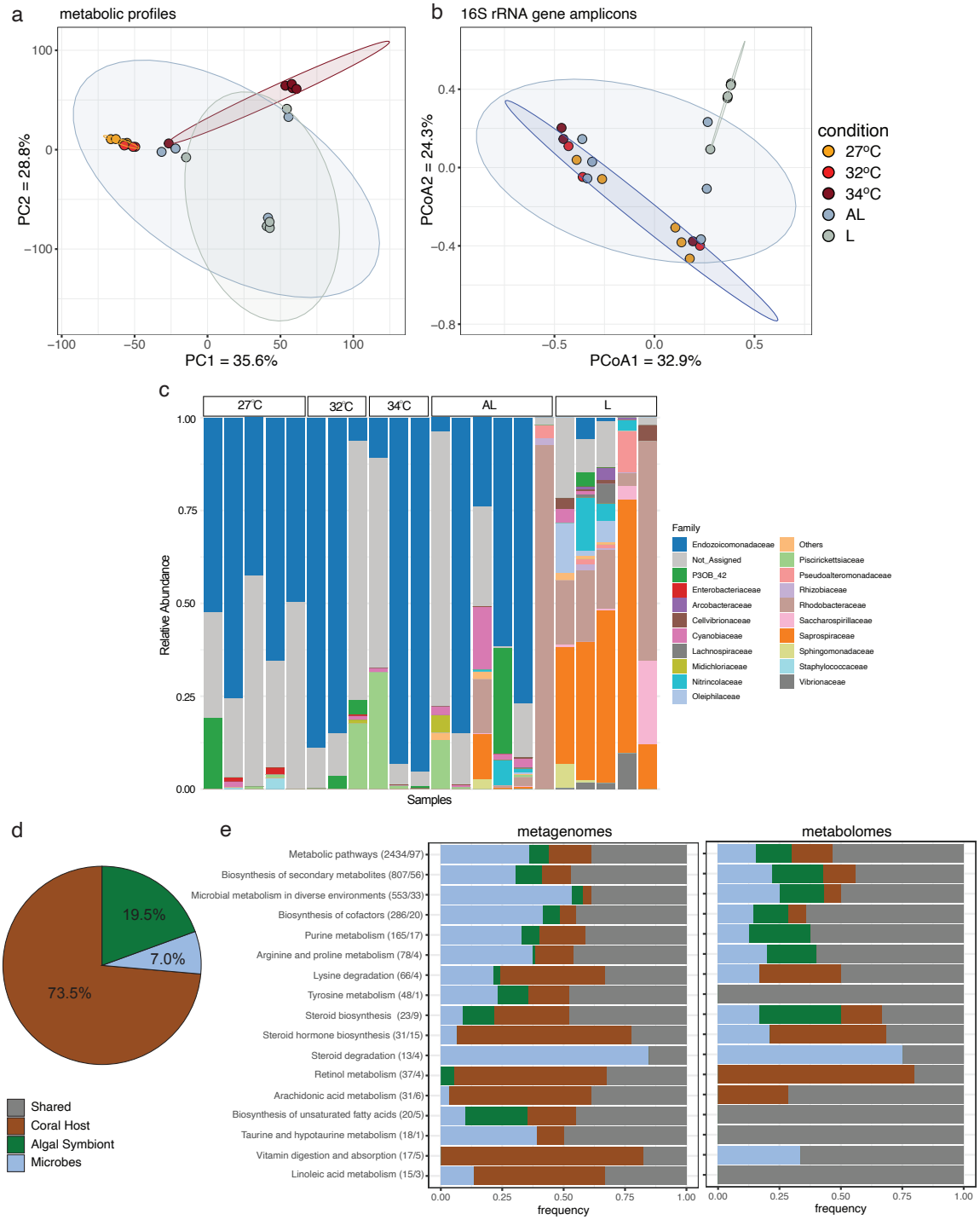

Figure 2. Integrated microbiome/metabolome analysis of the coral holobiont. a, Principal component analysis (PCA) of the metabolomics data (n=5878 putative molecular features). Samples collected at 27°C and 32°C cluster together and are significantly different from samples collected at 34°C. **b**, Principal coordinate analysis (PCoA) of microbial communities using Bray-Curtis distance shows significant differences between the diseased samples (i.e., AL and L) and all other samples. **c**, ASV-based bacterial community structure across temperatures and disease samples at the family level. Each bar plot represents the bacterial abundance of a coral colony.

692 The top 20 bacterial families are shown. **d**, Distribution of metagenomic reads from coral
693 holobiont metagenomes across coral, *Cladocopium spp*. (algal symbiont) and putative microbial
694 members. **e**, Distribution of host-algal symbiont-bacterial genes (left) and metabolites (right)
695 across the top-most abundant KEGG metabolic pathways. Numbers in parentheses refer to the
696 number of genes and metabolites shown in each pathway, respectively.

697

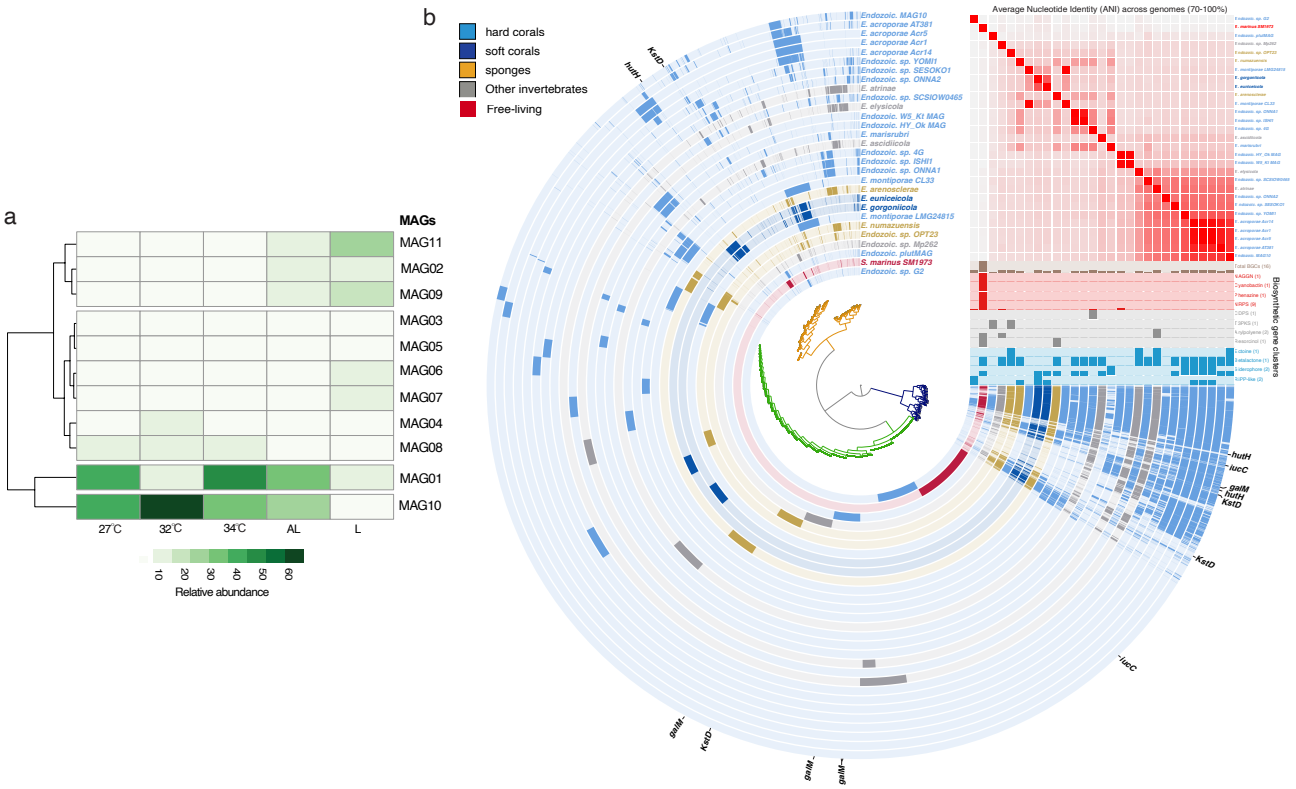

Figure 3. Abundance of *Endozoicomonas* MAG10 and the putative functional importance of *Endozoicomonas*. a, Relative abundance of tissue-associated MAGs inferred by read recruitment from metagenomes across all samples. Taxonomic classifications of MAGs are shown in SI Table 5. **b**, *Endozoicomonas* pangenome and biosynthetic gene clusters (BGCs) of 29 genomes and MAGs, including MAG10 and *E. acroporae* AT381. *Spartinivicinus marina* SM1973 was included to represent a free-living member of the Oceanospirillales as a close free-living isolate to *Endozoicomonas.* Pangenomic analyses based on the occurrence of gene clusters were implemented in Anvi'o[34]. The central dendrogram represents hierarchical clustering based on the presence (colored) or absence (opaque) of 34,846 gene clusters. Branches were colored based on core, accessory or singleton/doubleton genes. Each track in the pangenome represents a single genome colored according to its isolation source. Genomes were clustered based on their pairwise average nucleotide identity (ANI) values shown in the heatmap, which reveals high similarity between MAG10 and *E. acroporae* genomes. Distribution of BGCs across genomes is shown below the heatmap. Key genes related to aerobactin biosynthesis (*iucC*) and degradation of steroid hormones (*kstD*), galactose (*galM*), and histidine (*hutH*) are labeled on the periphery of the pangenome.

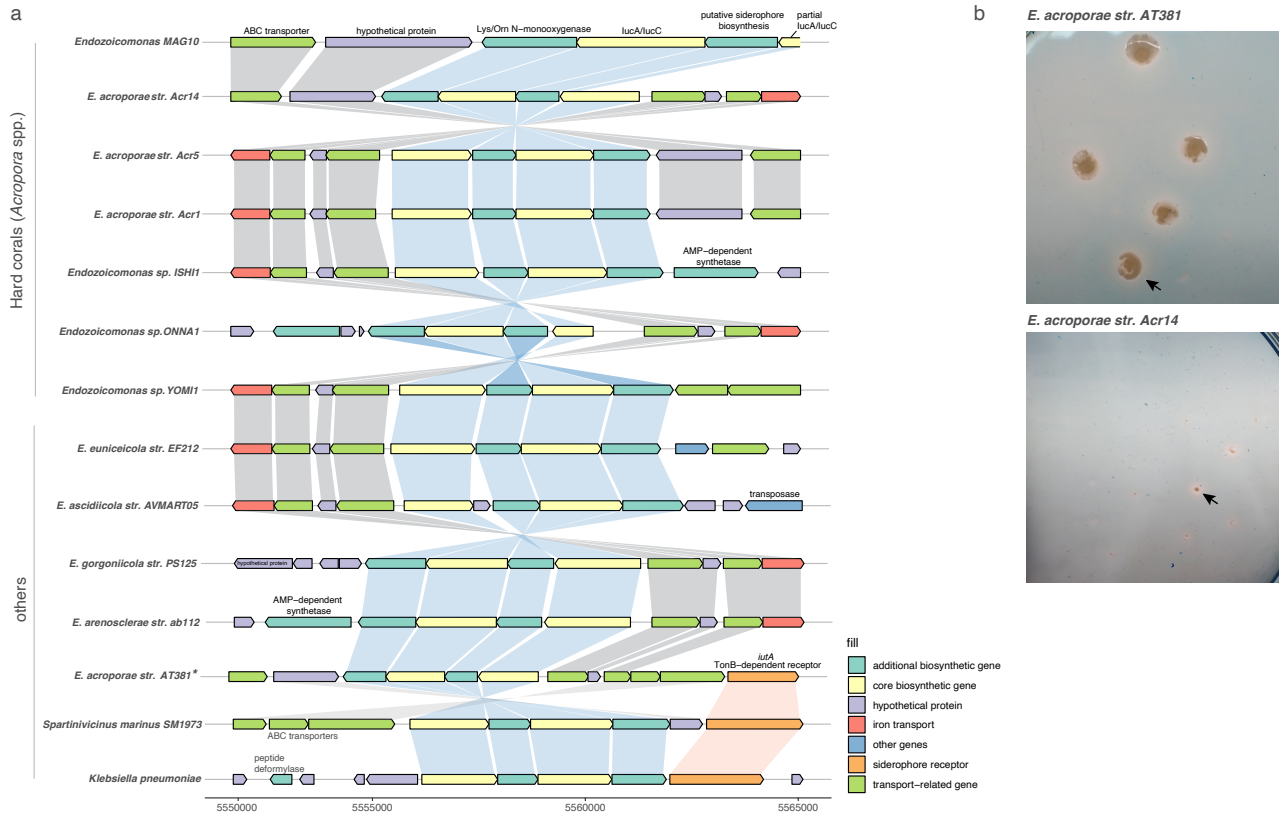

Figure 4. Utilization potential of the siderophore aerobactin for iron acquisition in *Endozoicomonas*. a, Genomic neighborhood organization of the aerobactin BGC in genomes of MAG10, *Endozoicomonas* spp. symbiotic with *Acropora* corals, soft corals, their closest free-living isolate, *S. marinus* SM1973, and the aerobactin-producer *Klebsiella pneumoniae*. Shading across genes represents gene synteny of aerobactin biosynthesis (blue), aerobactin uptake (orange), or other genes (grey). Aerobactin is biosynthesized by 4 genes, one of which is duplicated (*iucA/iucC*). Although the aerobactin biosynthesis operon is partially truncated in the MAG10 scaffold, we confirmed that the only partially truncated gene is the duplicated *iucA/iucC*. The TonB-dependent receptor refers to the aerobactin transporter gene, *iutA,* which is proximal to the BGC of SM1973 and K. *pneumoniae.* Among all coral-associated *Endozoicomonas,* only *E. acroporae* AT381 has *iutA* ~11kb distal to the BGC; all other *Endozoicomonas* genomes display a distal ortholog/paralog of *iutA* elsewhere in the genome (>11kb away from the biosynthesis BGC) **b**, CAS assay of cultures of two *E. acroporae* strains (AT381 and Acr14), encoding the aerobactin cluster, grown in iron-limited media on agar. Siderophore activity was then assessed through the formation of halos (black arrow) around bacterial colonies. * indicates isolation from hard coras from the genus *Acropora.*

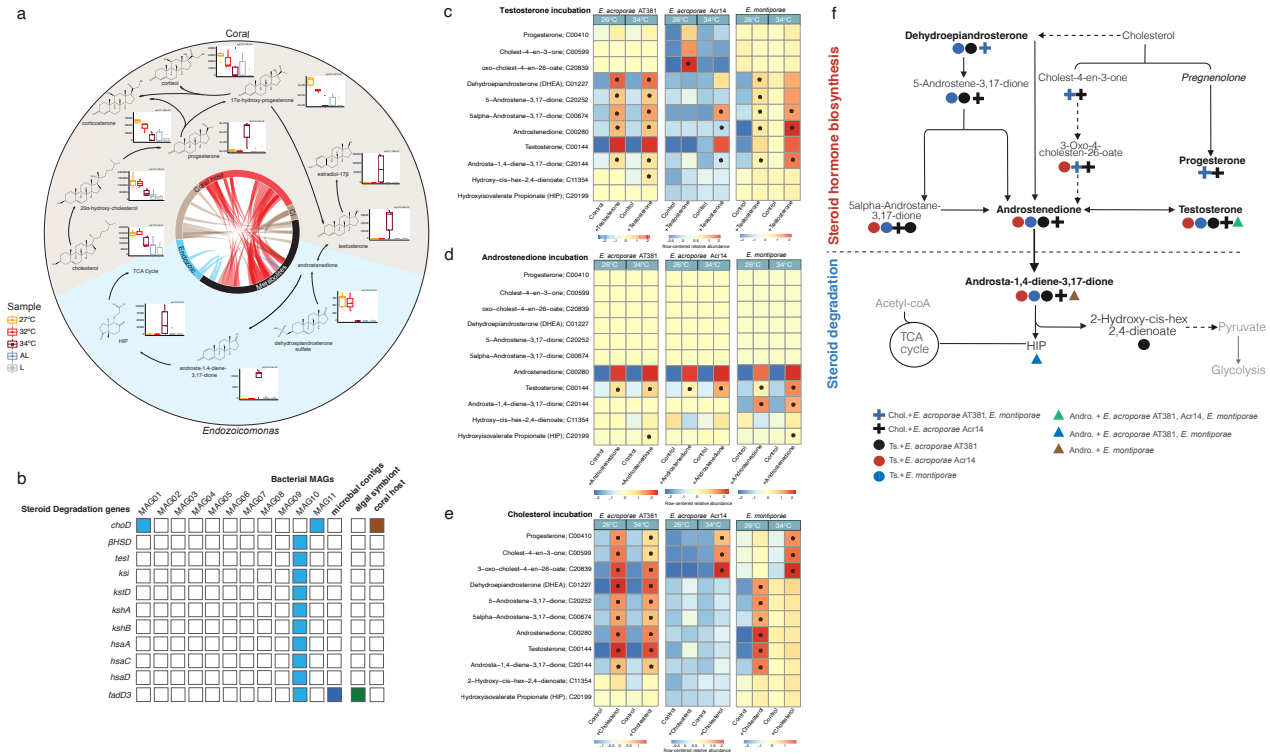

Figure 5. Putative steroid hormone biosynthesis/degradation in the holobiont across the temperature gradient and an abbreviated steroid hormone production pathway by *Endozoicomonas*. **a**, Steroid biosynthesis and degradation pathways based on coral and Endozoicomonas MAG10 contigs. Arrows indicate genes, and arrowheads correspond to the number of genes carrying a transformation. The relative abundance of putative steroid hormones is presented along with adjusted p-values, calculated using the Benjamini-Hochberg method, based on ANOVA results that assess the impact of temperature on changes in their abundance. Middle: Circos plot depicting all detected steroid-related metabolites and their connection to genes of *Endozoicomonas* (Endozoic.), the coral host, or *Cladocopium* spp. (Cl). The plot shows that steroid degradation is restricted to *Endozoicomonas*, steroid biosynthesis is mostly dominated by *Cladocopium* and steroid hormone biosynthesis is mostly dominated by the coral. Colors indicate different pathways (brown=steroid biosynthesis, red=steroid hormone biosynthesis, blue=steroid degradation, black=metabolites). **b**, Presence/absence of steroid degradation genes in the holobiont. Note that microbial contigs excluded contigs used to construct the bacterial MAGs. cholesterol oxidase; choD, beta-hydroxysteroid dehydrogenase; βHSD, 3-oxo-5alpha-steroid 4-dehydrogenase; tesI, steroid Delta-isomerase; ksi, 3-oxosteroid 1-dehydrogenase; kstD, 3-ketosteroid 9alpha-monooxygenase subunit A; kshA, 3-ketosteroid 9alpha-monooxygenase subunit B; kshB, 3-hydroxy-9,10-secoandrosta-(10)1,3,5-triene-9,17-dione monooxygenase; hsaA, 3,4-dihydroxy-9,10-secoandrosta-(10)1,3,5-triene-9,17-dione 4,5-dioxygenase; hsaC, 4,5:9,10-diseco-3-hydroxy-5,9,17-trioxoandrosta-2,(10)1-diene-4-oate hydrolase; hsaD, HIP-CoA ligase; fadD3. **c, d and e,** Steroid hormone production by three *Endozoicomonas* strains. Two *E. acroporae* (AT381 and Acr 14) and one *E. montiporae* strains were incubated with or without testosterone (**c**) , Androstenedione (**d**), or cholesterol (**e**), at 26°C and 34°C. Heatmaps show the normalized mean relative abundance of each metabolite in each condition, with * indicating statistical significance of their treatment relative to controls (T-test, adjusted p-value <0.05). Statistical significance was not calculated for

761 testosterone/androstenedione in **c, d** because both were added to the media. All detected
762 metabolites were annotated based onaccurate mass within 5 ppm and high-resolution MS/MS
763 fragmentation of standards. Additionally, a testosterone standard was used to further confirm its
764 production using the aforementioned criteria and retention time. **c,** Novel pathway for the
765 production of progesterone and testosterone inferred from metabolomics analysis. Dotted lines
766 indicate the absence of genes involved in these specific metabolic reactions in the
767 *Endozoicomonas* genomes.

768

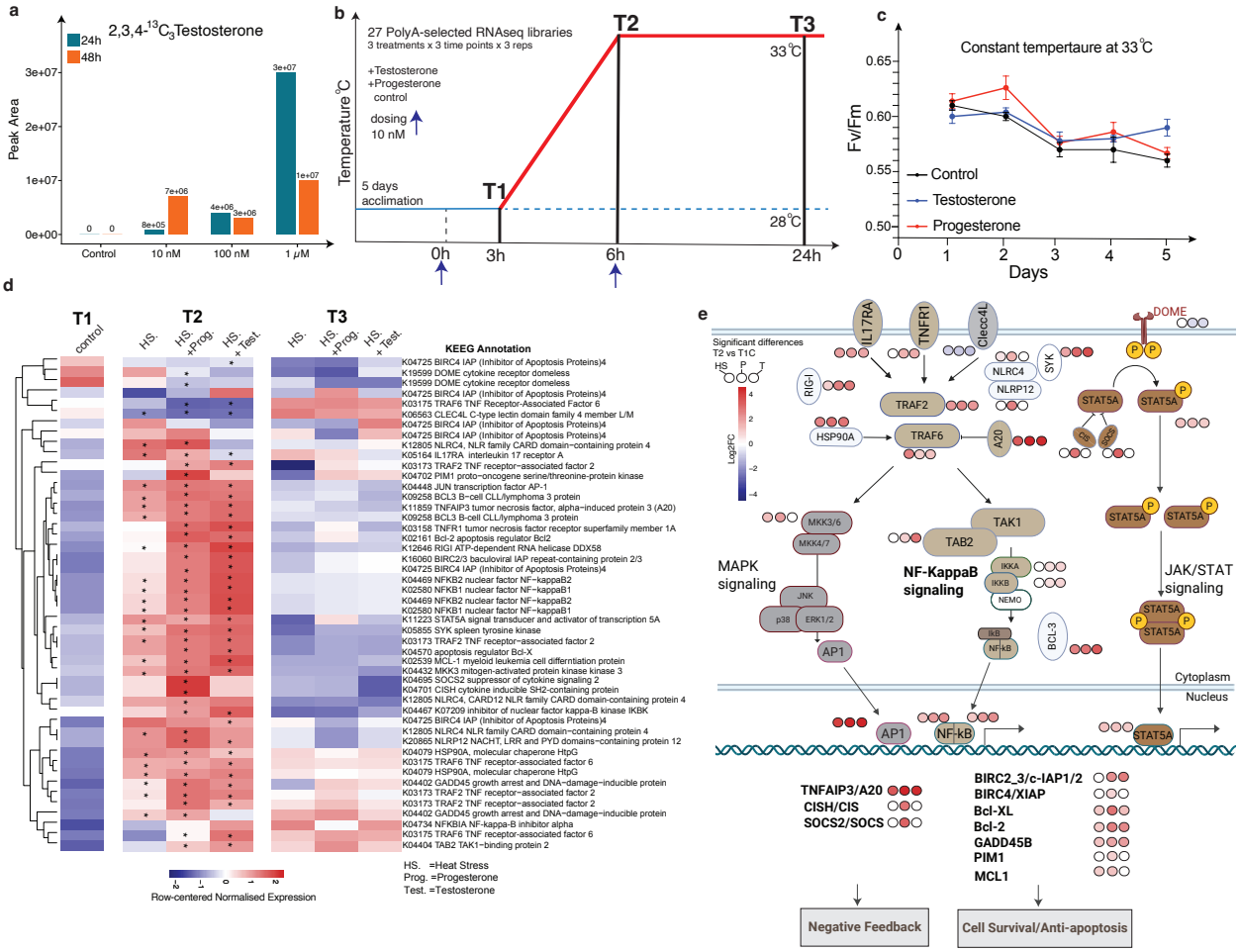

Figure 6. Activation of the coral innate immune response by progesterone and testosterone during heat stress. a, Uptake and accumulation of ^{13}C-labeled testosterone in coral tissues over a 48-h exposure period. Peak area was normalised to dry extract weight. **b**, Experimental design. *Acropora* colonies were exposed to acute thermal stress with or without the addition of progesterone or testosterone. Hormones were administered at 10 nM at the start of the experiment at 28°C. Three hours later, the first sampling point (T1) was collected for RNA-seq analysis, followed by a second hormone dose at 6 h. The temperature was ramped up from 28°C to 33°C over 3 h after T1 collection, and samples were collected at T2 along with untreated controls. Final sampling (T3) was conducted after 24 h of exposure at 33°C. **c**, Maximum quantum yield of photosystem II (F_v/F_m) was measured daily as an indicator of photophysiological stress and a proxy for the coral holobiont health. **d**, Heatmap showing normalized expression levels of selected immunity-related genes differentially regulated across treatments and time points. Significantly differentially expressed genes at 6 hours compared to controls (FDR < 0.05) were highlighted by asterisks. All differential expressions were based on biological triplicates. **e**, Pathway diagram based on KEGG annotations highlighting genes associated with innate immune pathways, including immune receptors, intracellular signaling cascades, and downstream effector responses. Tumor necrosis factor receptor 1 (TNFR1), TNF receptor–associated factor 2 (TRAF2), TNF receptor–associated factor 6 (TRAF6), TAK1-binding protein 2 (TAB2), Mitogen-activated protein kinase kinase 3 (MKK3), Mitogen-activated protein kinase kinase 4/7 (MKK4/7), Nuclear factor kappa-B subunit 1/2 (NFKB1/2), NF-κB inhibitor alpha (IκBα / NFKBIA), Inhibitor of nuclear factor κB kinase subunit alpha/beta

791 (IKBKA/B), NF-κB essential modulator (NEMO / IKBKG), Activator protein 1 (AP-1), C-type lectin
792 domain family 4 member L (CLEC4L), Retinoic acid–inducible gene I (RIG-I), Interleukin-17
793 receptor A (IL17RA), Signal transducer and activator of transcription 5A (STAT5A), Cytokine
794 receptor domeless (DOME), Spleen tyrosine kinase (SYK), B-cell lymphoma 2 (*BCL2*), B-cell
795 lymphoma extra-large (*BCL-XL*), baculoviral IAP repeat-containing proteins 2 and 3 (*BIRC2/3*),
796 tumor necrosis factor alpha–induced protein 3 (*TNFAIP3*), cytokine-inducible SH2-containing
797 protein (*CISH*), suppressor of cytokine signaling 2 (*SOCS2*), heat shock protein 90 alpha
798 (*HSP90A*).

799

800